Downloaded from gsabulletin.gsapubs.org on May 3, 2012

Transport and deposition of a pyroclastic surge across an area of high relief: The 18 May 1980 eruption of Mount St. Helens, Washington

RICHARD V. FISHER *Department of Geological Sciences, University of California, Santa Barbara, California 93106*

ABSTRACT

The 08:32 PDT 18 May 1980 Mount St. Helens eruption began as an explosion (blast) that produced a laterally flowing pyroclastic current (blast surge). It moved outward in a 180° arc at supersonic speeds and then slowed to subsonic speeds. Supersonic flow severely eroded the ground and produced a ground layer (formerly, layer A0). Above the ground layer lies the deposit derived from the blast surge.

The blast surge deposits formed in three continuous and concurrent stages. The first stage was movement of the *transport system* (that is, the blast surge), carrying fragments most of the distance from the vent. The next two stages involved the *depositional system.* This system developed from rapidly accumulating sediment by gravity segregation at the base of the blast surge. Two stages of sediment gravity flows with independent flow regimes formed sequentially in rapid succession from the moving blast surge. Each moved downhill due to gravity, independently of the generating blast surge that was driven by explosive expansion. Units repeated in some sections are deposits derived from divergent and crossing surge lobes caused by irregular topography. Locally ponded massive deposits in valleys and depressions formed from gas-rich pyroclastic flows and originated in two ways: (1) topographic *blocking* by steep, volcano-facing slopes. Blocking includes diversion or damming of the lower-elevation, high-density part of the blast surge that could not surmount high ridges. (2) Also occurring to form valley ponds was *drainage* of just-deposited (or "almost deposited") material from steep slopes (>~30°–35°), moving downhill in all slope directions into separate valleys or depressions.

Distances traveled by the blast surge, and rates at which coarsest fragments decrease laterally, are related to the topographic "grain." Surge runout was farther where flow directions paralleled topographic trends, and least where trends were at right angles to the flow. Obstacle-interference depositional patterns (thinning-thickening; rapid fine-to-coarse facies changes) caused a spread in median diameter values that are as great in local areas near the volcano as they are over the width of the devastated region.

INTRODUCTION AND PREVIOUS WORK

The 08:32 Pacific Daylight Time 18 May 1980 blast from Mount St. Helens, Washington, a northward-directed explosion, produced a high-velocity, particle-rich flow. The current was probably turbulent (therefore defined as a surge) and density stratified (Valentine, 1987). It was modeled as an overpressured jet (Kieffer, 1981). The word "blast" has been used to describe the explosion; therefore, the term "blast surge" is used to signify the consequent current (Fisher and others, 1987). A blast surge is a special type of pyroclastic surge, as are base surge, ash-cloud surge, and ground surge (Fisher and Schmincke, 1984). The distribution of the blast deposits is shown in Figure 1.

The blast surge deposits consist of accidental, accessory and juvenile, fine- to coarse-grained ash, lapilli, and blocks. Accidental materials are mainly basaltic to dacitic volcanic rocks and granitic intrusive rocks from the Tertiary basement (Evarts and others, 1987) and dacitic pumice from pre–1980 Mount St. Helens' eruptions picked up by the blast surge. The accessory fragments are andesite, dacite, and subordinate basalt from the edifice of the volcano. The juvenile material is called "blast dacite." It is commonly light gray, poorly vesiculated, prismatically fracturing material derived from the cryptodome that produced the blast (Hoblitt and others, 1981). Dark gray blast dacite also occurs (R. P. Hoblitt, 1987, personal commun.).

The multilayered deposit resulting from the blast surge (Hoblitt and others, 1981; Moore and Sisson, 1981; Waitt, 1981; Fisher and others, 1987; Brantley and Waitt, 1988) covers an area of about 600 km^2. This report considers most of the devastated area from the North Fork Toutle River northward in an arc extending to the eastern margin of the deposit, using data gathered from about 420 measured sections, many of which are located in Figure 1. The area south of the North Fork Toutle River was not included in the study. All distance measurements herein are from the center of the crater of Mount St. Helens.

The initiating avalanche and subsequent blast on May 18, 1980, has been well described by others (Glicken, 1986, and in press; Voight, 1981; Voight and others, 1981, 1983). The blast, following the debris avalanche, had an initial velocity of 90–110 m s^{-1} (Voight, 1981) but may have increased to a maximum of 325 m s^{-1} due to lateral expansion (Kieffer, 1981; Moore and Rice, 1984). Based upon dimensions of erosional furrows, the blast had an estimated velocity of 235 m/s in the area of Johnston Ridge (Kieffer and Sturtevant, 1988). Moore and Rice (1984) suggested that there was a second explosion originating in Spirit Lake, but this source is not indicated by depositional units in the study area.

The purpose of this study is to determine the causes and mechanisms by which the Mount St. Helens blast surge deposited several layers of tephra (Hoblitt and others, 1981; Moore and Sisson, 1981; Waitt, 1981; Fisher and others, 1987), apparently from one explosion (blast), but possibly from two blasts (Hoblitt, 1988,

Geological Society of America Bulletin, v. 102, p. 1038–1054, 25 figs., 1 table, August 1990.

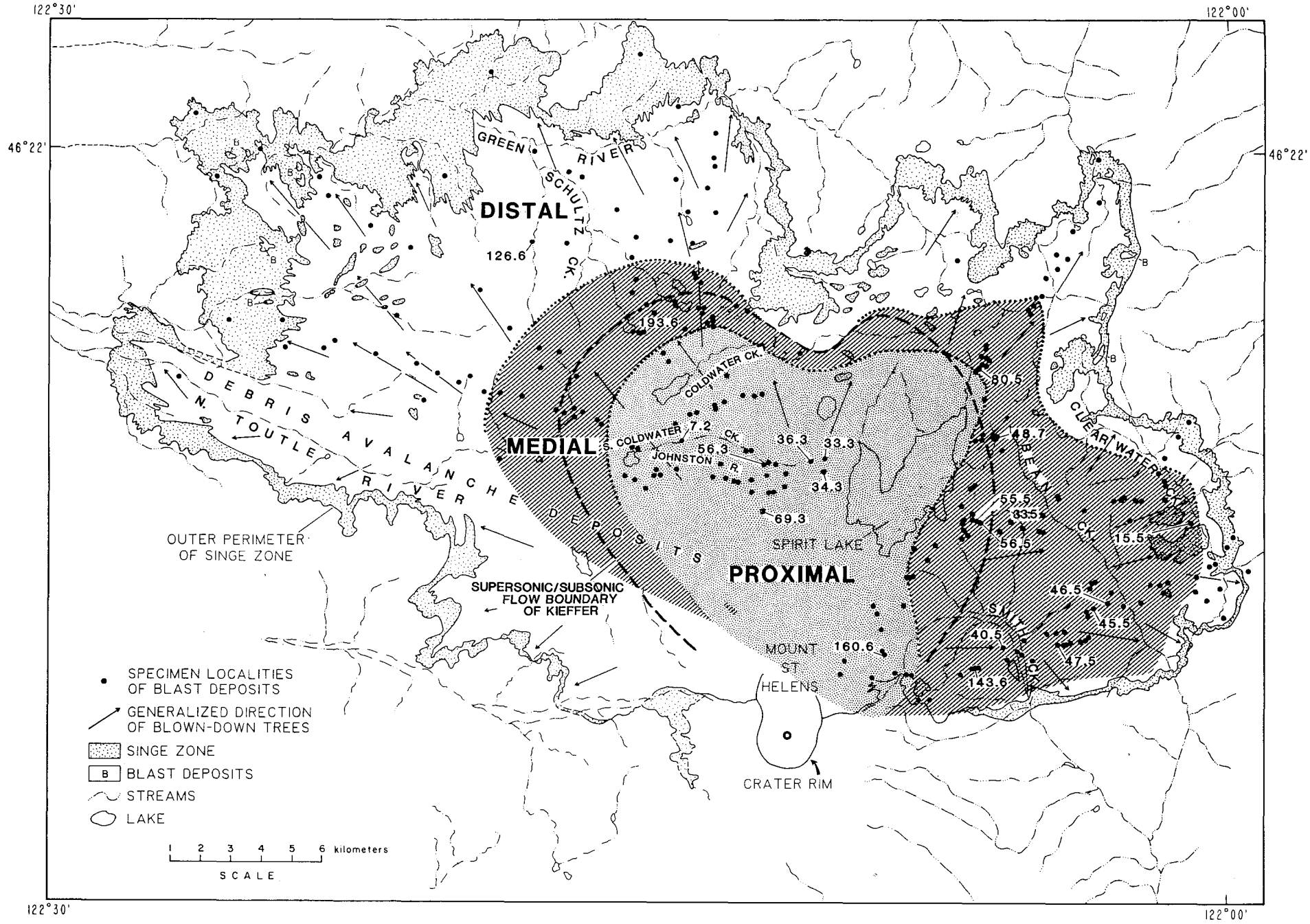

Figure 1. Index map showing area of blast deposits and location of measured sections (filled circles). Numbered localities are those referred to in text. Arrows show generalized tree blowdown directions. Proximal, medial, and distal zones are patterned. Generalized from Lipman and Mullineaux (1981, p. I).

Downloaded from gsabulletin.gsapubs.org on May 3, 2012

1989), and to explain the effects of topography upon the deposition of materials from pyroclastic surges.

STRATIGRAPHY AND DEPOSITIONAL ZONES

Introduction

The area covered by the Mount St. Helens blast surge is divided here into three major zones: proximal, medial, and distal. The boundary between the zones approximately parallel the calculated boundary (Kieffer, 1981) between supersonic and subsonic flow (Fig. 1). There are five main depositional units within these zones that were derived from the eruptive activity between 8:32 and about 10 a.m. of May 18, 1980 (Criswell, 1987). The lowest layer of the blast-related sequence is here called a "ground layer" which was derived from interaction of the moving blast surge with the ground (originally called "layer A0" by Fisher and others, 1987), overlain by layers A1, A2 (deposited from the blast surge) (Fig. 2), A2* (derived from mixing of layers A1 and A2), and A3 (a fallout layer).

Layers A1 and A2 were deposited directly from the blast surge (Waitt, 1981; Hoblitt and others, 1981; Moore and Sisson, 1981; Fisher and others, 1987). Layer A1 differs from layer A2 by its lighter gray color and lower percentage of fines (average = 4.9%; Table 1). The term "fines" refers to fine-grained ash less than 1/16 mm in diameter (>4 phi). Layer A2 contains a greater percentage of fines (average = 14.4%) than does layer A1, which causes it to be more cohesive than layer A1 and yellow to yellow-gray in color. The fines that characterize layer A2 have oxidized since 1980; layer A2 was initially olive-gray. Starting in about 1983, the color change accelerated. Locally, there are additional interbedded gray, fines-poor, medium- to coarse-grained ash layers at variable stratigraphic horizons below and between layers A1 and A2.

All units that resulted from lateral movement (the ground layer and layers A1, A2, and A2*), are capped by layer A3, a fallout layer with abundant accretionary lapilli (Hoblitt and others, 1981; Moore and Sisson, 1981; Waitt, 1981; Sisson, 1982; Sparks and others, 1986).

Proximal Zone

The proximal zone (Fig. 1) is defined as the area where there is more erosion of the ground surface than in other zones, and the duff (that is, the organic forest litter) was removed from unprotected areas facing the volcano. The thickest and coarsest deposits occur in this zone. The proximal zone extends outward to a maximum of about 11 km.

TABLE 1. SIZE, SORTING, AND FINE ASH % FOR BLAST SURGE LAYERS

	Northwest	North	East	All samples
MEDIAN DIAMETER AVERAGES	Average (number of samples) {Lowest and highest values}			
Layer A2b	2.3 (26) {0.9–2.8}	2.1 (31) {0.9–2.8}	2.0 (50) {0.7–2.6}	2.1 (107) {0.7–2.8}
Layer A2a	1.9 (29) {1.0–2.6}	1.5 (31) {0.7–2.5}	1.7 (49) {0.0–2.6}	1.7 (109) {0.0–2.6}
Layer A1	1.3 (31) {0.3–2.0}	1.1 (33) {0.2–1.9}	0.9 (90) {–0.1–2.6}	1.1 (154) {–0.1–2.6}
Ground layer	1.3 (21) {0.9–1.9}	1.0 (22) {0.1–1.3}	0.8 (36) {0.0–2.1}	1.0 (79) {0.0–2.1}
SORTING AVERAGES				
Layer A2b	1.3 (26) {0.9–1.8}	1.4 (31) {0.9–1.8}	1.4 (50) {1.0–1.9}	1.4 (107) {0.9–1.9}
Layer A2a	1.5 (29) {1.1–1.8}	1.6 (31) {1.2–1.9}	1.5 (48) {1.0–1.9}	1.5 (108) {1.0–1.9}
Layer A1	1.7 (31) {1.2–2.0}	1.7 (33) {1.3–2.1}	1.6 (85) {1.0–2.1}	1.7 (149) {1.0–2.1}
Ground layer	1.7 (21) {1.3–2.0}	1.7 (22) {1.5–1.9}	1.7 (33) {1.4–2.0}	1.7 (76) {1.3–2.0}
PERCENT FINE ASH AVERAGES				
Layer A2b	22.6 (26) {5.0–34.7}	19.6 (31) {4.0–33.8}	10.8 (50) {0.4–23.6}	17.7 (107) {0.4–34.7}
Layer A2a	14.0 (29) {4.4–32.1}	10.8 (31) {3.2–35.6}	8.3 (49) {1.4–24.8}	11.0 (109) {1.4–35.6}
Layer A1	6.3 (31) {2.2–12.8}	5.7 (33) {0.9–19.4}	2.8 (90) {0–13.9}	4.9 (154) {0–19.4}
Ground layer	7.8 (21) {4.0–14.1}	5.0 (22) {2.0–8.5}	6.0 (36) {0.7–32.3}	6.3 (79) {0.7–32.3}

Note: all numbers are in phi units. Fine ash is <4 phi. Number of samples in parentheses; lowest and highest values in braces.

Ground Layer. The ground layer in the proximal zone consists of from one to as many as five beds. Many beds are poorly sorted mixtures of uncharred organic fragments and soil schlieren from the ground surface mixed with 0 to ~5% juvenile dacite (Fisher and others, 1987). Some beds contain pre–1980 pumice and ash, and others consist of reworked underlying soil or Tertiary rocks. In one place, the ground-layer interval consists of finger-like injections of a mixture of soil and blast-dacite fragments into an unconsolidated underlying pumice formation (Fig. 3).

Woody organic debris in the ground layer is more abundant than in layer A1 across the region in all of the zones and usually is not charred or burned. In places where tree limbs project from it into layer A1 above, the wood is charred only in layer A1.

In several outcrops between the North Fork Toutle River and the southern base of Johnston Ridge, the blast-surge material is ponded to form a thick layer, A2*. Dark gray to reddish hummocks from Slide Block I (Fisher and others, 1987) commonly rest upon Tertiary volcanic rocks. The avalanche hummocks dammed south-flowing tributaries of the North Fork Toutle River, causing ponding of blast-surge material behind the dams. Between some hummocks and above others, the ground layer is pale orange and consists of as many as three beds (Fig. 1, locality N69.3). At other places (Figs. 1 and 4, locality N56.3), the ground layer consists of as many as five beds.

The proximal sections of the ground layer have in common (1) the presence of lenticular fines-poor layers containing blast dacite (similar to layer A1), commonly mixed with noncharred wood, and overlain by blast-dacite–poor, organic-rich layers; (2) layers with clots of soil schlieren; and (3) layers containing ground-surface debris that is poorly mixed with a small percentage of blast dacite.

A basal turbulent boundary layer of the blast surge head and strong shearing action on soil, rock, and vegetation are believed to be the dominant mechanisms by which the ground layer originated in the proximal zone. The 1% to 5% of juvenile blast dacite that is mixed within some of the beds of the ground layer may have been derived from the blast that penetrated and mixed with the headwall of Avalanche I (Voight, 1981). Layers consisting of up to 57% blast dacite are present, which suggests a possible early explosive pulse of the blast as has been reported by Hoblitt (1988, 1989). Another explanation is suggested by relationships at locality N34.3 (Figs. 1 and 5) within a furrow where a dacite-

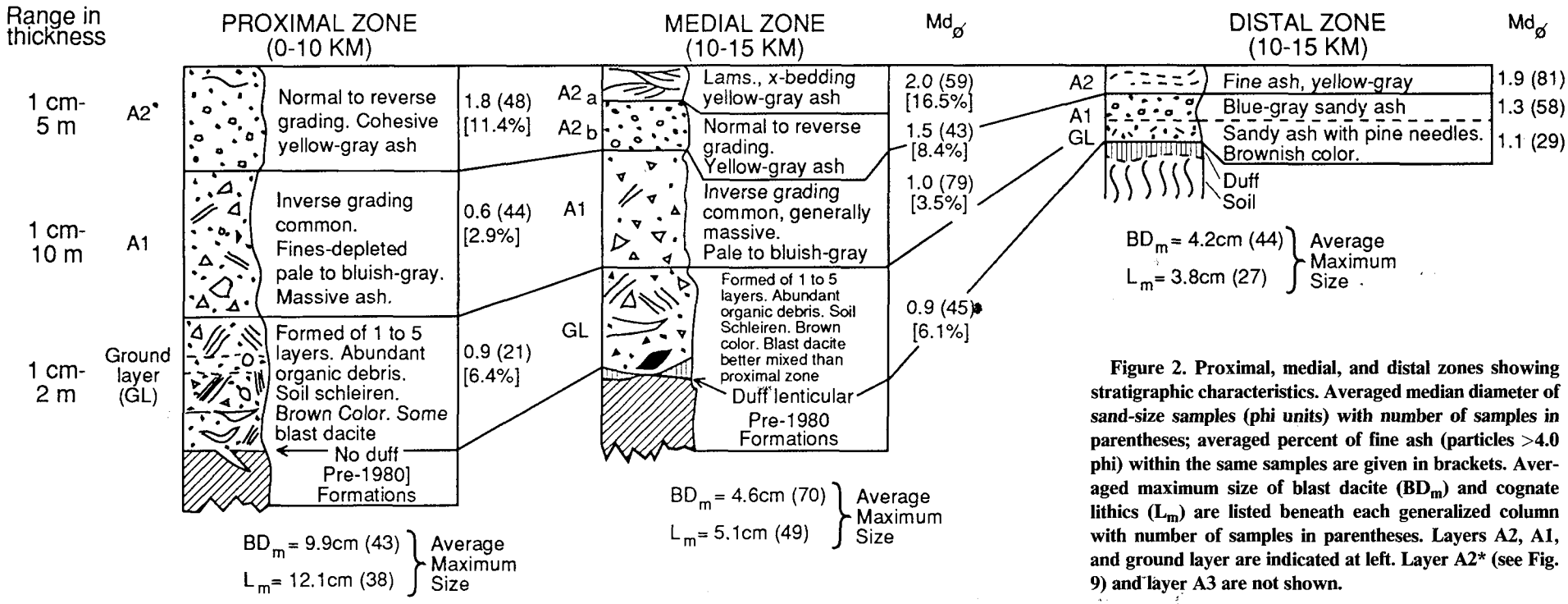

Figure 2. Proximal, medial, and distal zones showing stratigraphic characteristics. Averaged median diameter of sand-size samples (phi units) with number of samples in parentheses; averaged percent of fine ash (particles >4.0 phi) within the same samples are given in brackets. Averaged maximum size of blast dacite (BD_m) and cognate lithics (L_m) are listed beneath each generalized column with number of samples in parentheses. Layers A2, A1, and ground layer are indicated at left. Layer A2* (see Fig. 9) and layer A3 are not shown.

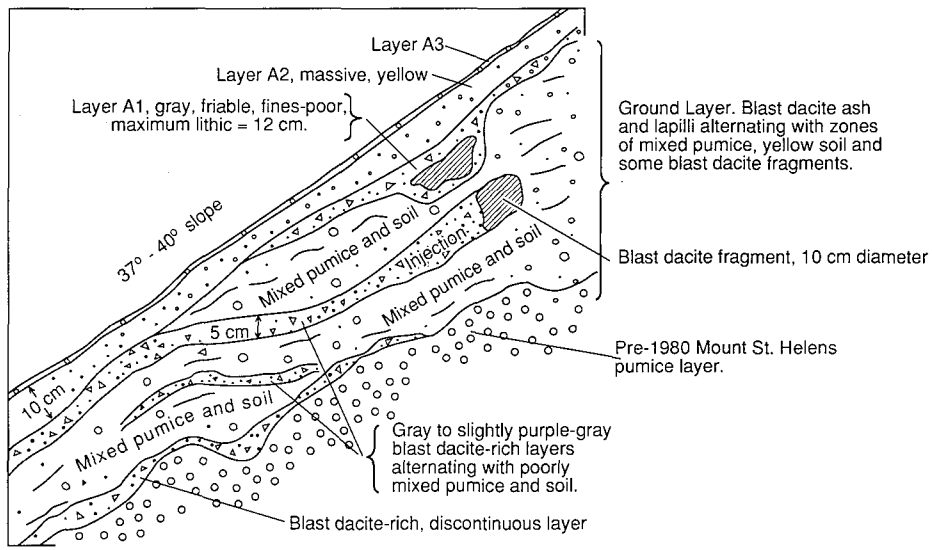

Figure 3. Locality E160.6. Small finger-like dikes of purplish to reddish-gray, blast-dacite–rich tephra intrude an unconsolidated mixture of pre–1980 pumice tephra, soil, and some blast dacite. Sequence suggests that blast surge head plowed into the soil and the pumice layer, mixing it with soil and blast dacite, followed by injection of more blast-dacite–rich material from the surge head into the ground layer. This was followed by emplacement of layers A1, A2, and A3. Flow direction was to the right.

Downloaded from gsabulletin.gsapubs.org on May 3, 2012

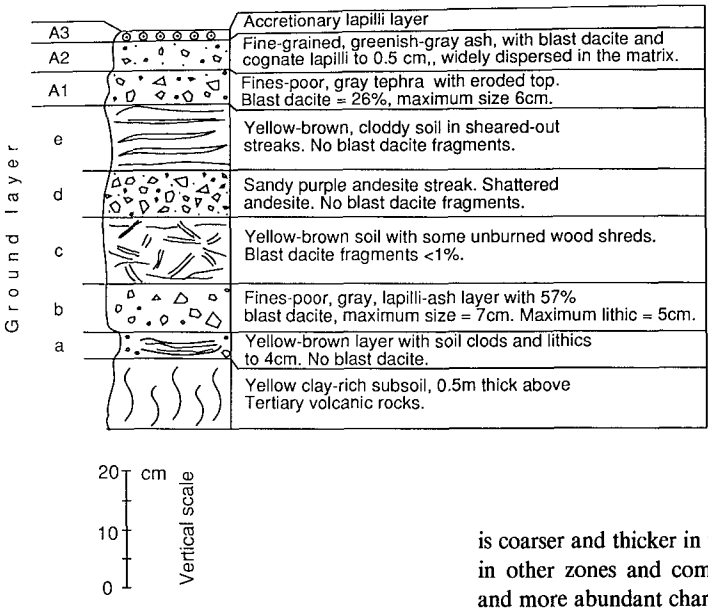

Figure 4. Locality N56.3, 8.8 km from crater of Mount St. Helens about halfway down the north side of Johnston Ridge. Ground layer consists of five beds. The lowest 5-cm bed of the ground-layer sequence is composed of a sheared yellow-brown soil similar to the soil beneath the section. This is followed by a fines-poor blast-dacite–rich (57%) bed similar to layer A1. There is a trace of blast-dacite fragments in layer c, but it is lacking in layers d and e.

rich, fines-poor layer occurs at the base of the section. Deposition of this layer may have been caused by vortical motion (Kieffer and Sturtevant, 1988), rotating material from within the head of the blast surge to the ground surface during erosion of the furrow.

Layer 1. This layer is a massive, friable, bluish-gray lithic volcanic rubble to coarse-grained ash with a small amount of fine-grained ash, usually without internal bedding. Layer A1 is coarser and thicker in the proximal zone than in other zones and commonly contains larger and more abundant charred wood fragments. It is thickest in valley bottoms, in the lee of obstacles, and at many localities on the lower slopes of ridges facing the volcano (Fisher and others, 1987). Blast dacite occurs in varying percentages (about 20%–50%). Layer A1 commonly shows reverse-to-normally graded lapilli- to block-sized fragments of variable vesicularity supported within a coarse, fines-poor, ash matrix.

The contact of layer A1 with the overlying layer A2 is commonly sharp, but in some localities, there are hundreds of pipe-like structures of fines-poor, blast-dacite ash extending upward into the base of layer A2 (for example, locality N33.3, Fig. 6). These are interpreted to be tiny gas pipes.

Layer A2. Within the proximal zone, this layer is characteristically massive, is either normally or reversely graded, and contains dispersed matrix-supported blast-dacite lapilli. In the proximal zone, however, in the lee of obstacles (tree stumps, large boulders, and ridge crests), the top few centimeters of layer A2 has wavy laminations and is finer grained than all layers beneath it.

The contact relationship between layer A2 and A1 suggests that layer A1 was gas-rich during transport, but because it lacked abundant fines and thus was permeable, gases were usually expelled quickly during transport. Except in a few places, gas loss occurred before layer A2 was fully in place, allowing development of a sharp contact by movement of A2 after A1 had come to rest. At a few localities, however, layer A2 was emplaced fast enough to seal off the gas within layer A1 before it completely escaped, and the gas pressure was great enough to cause continued upward movement of gas into layer A2, resulting in preservation of the gas pipes.

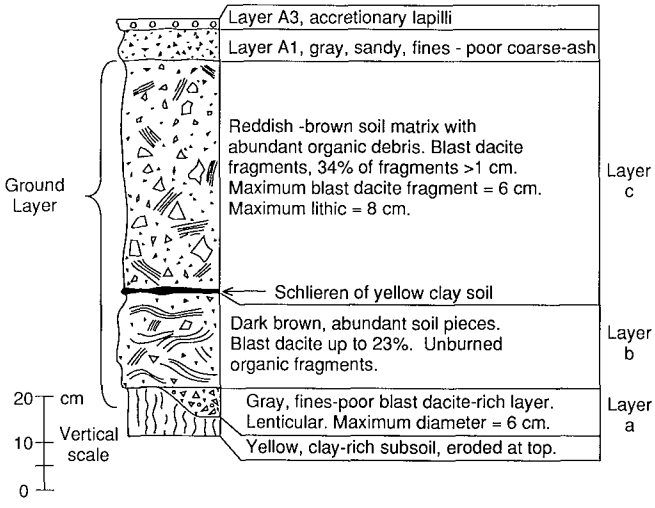

Figure 5. Locality N34.3, relatively thick ground layer (70 cm), 8.4 km from volcano in U-shaped furrow. The lowest layer is a lenticular, dacite-rich layer of fines-poor, medium- to coarse-grained ash. Above it is a poorly mixed and sheared soil zone containing unburned organic debris, which is overlain by a reddish-brown, well-mixed layer containing abundant organic material and 34% blast-dacite fragments for sizes larger than 1 cm. The ground layer is overlain by fines-poor layer A1, 7 cm thick.

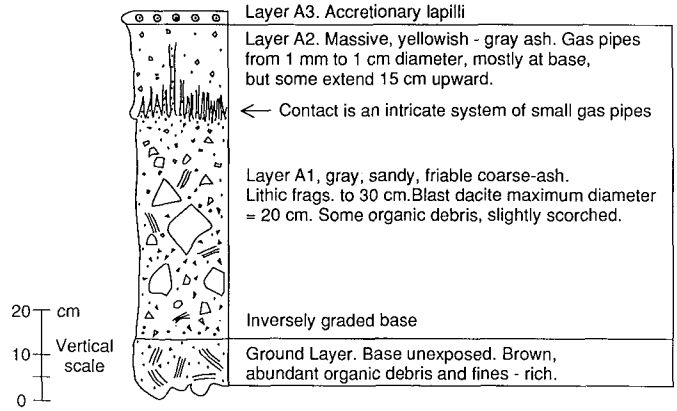

Figure 6. Locality N33.3, 9.5 km from source. Upper contact of layer A1 shows innumerable tiny gas pipes extending upward into layer A2.

Downloaded from gsabulletin.gsapubs.org on May 3, 2012

Medial Zone

The medial zone has some of the features of both the proximal and distal zones (Fig. 2). It is the area in which the duff layer is eroded discontinuously in open areas facing the volcano. The medial zone is 1–4 km wide to the northwest and north, but to the east, it is about 11 km wide and appears to extend almost to the singe zone of the blast surge in that direction.

Ground Layer. The ground layer of the medial zone is thinner than in the proximal zone, and debris (soil, organic material, juvenile and cognate fragments) that makes up the layer tends to be somewhat better mixed.

Layer A1 in the medial zone is similar to A1 in the proximal zone, but it is thinner and finer grained.

Layer A2 in the medial zone consists of two parts, (1) a massive lower layer (layer A2a), commonly with poorly developed reverse-to-normal grading, and (2) an upper part (layer A2b) that is finer grained than A2a, laminated, cross-bedded, and locally has well-formed dunes. Layer A2 begins to differentiate into two layers within protected parts of the proximal zone, and the two layers are well developed in nearly all localities of the medial zone.

In some places within the medial zone, blast surge material is entirely absent, and layer A3 lies directly upon the pre-eruption ground surface. These areas are discussed in a section below titled "islands of nondeposition."

Distal Zone

The distal zone is the area beyond about 16 km to the northwest and north, extending to the edge of the devastated area. It is the area where the soil and overlying duff are not significantly eroded and where deposits are thinner and finer grained than elsewhere (Fig. 2).

The *ground layer* in the distal zone thins to an average of about 10 cm or less (down to 1 cm) and consists in most places of coarse ash well mixed with small (2-mm to 5-mm) cognate to juvenile lapilli and abundant small twigs and pine needles. Light gray blast dacite forms about 20%–25% of the layer. Evidence of strong shearing and mixing with underlying soils is not evident.

Improvement of mixing of ground material and blast dacite begins at irregular distances from the volcano within the medial zone. Mixing becomes more thorough in the distal zone beyond about 15 km to the north and northwest. In the distal zone, the ground layer rests with little erosion upon the easily erodible forest litter beneath it. This suggests that low-density organic debris, consisting mostly of pine needles, was picked up from the duff but was prevented from being carried upward into the blast surge. Most of the picked-up organic debris apparently remained within the developing ground layer, suggesting that a thin turbulent zone of mixing developed on the ground surface at the base of the blast surge prior to deposition of layers A1 and A2.

In the inner sourceward part of the distal zone, layer A1 is thinner than in most places of the proximal and medial zones, and in some places, it is laminated. In outer distal areas, it is a thin (1- to 2-cm-thick), gray, medium- to coarse-ash layer with a few blast-dacite lapilli up to 1.5 cm in diameter and no internal laminations.

Layer A2, in the inner sourceward part of the distal zone, is composed of a massive lower part (A2a) and a laminated upper part (A2b). In some places on steep lee slopes, however, layer A2a has a crude wavy bedding and is segregated into coarse- and fine-grained laminations. In the outermost distal zone, between 2 to 5 km from the singe zone, the two-part division of layer A2 disappears, and it becomes a single, fine-grained, thin (1- to 2-cm), massive layer.

Layer A2*

Layer A2* (Fisher and others, 1987) is a poorly sorted deposit without internal layering that rests upon layers A1 and A2 and is overlain by layer A3. The layer is discontinuous, and it is most abundant in proximal areas, occurring in small basins within the headwaters of tributary valleys, cirques, and in the valleys of Smith Creek (Brantley and Waitt, 1988), South Coldwater Creek, in the lower part of Coldwater Creek (now covered by lake water), in upper North Fork Toutle River, and in a tributary of Schultz Creek of the Green River watershed, which is in the distal zone. Most distal valleys lack deposits of A2*.

The Schultz Creek tributary exposure of layer A2* (locality N126.6) occupies an elongate area of about 0.5 km^2. There, the base of A2* lies upon layers A1 and A2, which in turn rest upon pre-eruption terrace gravels (Fig. 7).

There are abundant gas pipes almost totally depleted in fine-grained tephra (<4% fine ash) within the thickest ponds of layer A2*, which are in the proximal zone at the southern base of Johnston Ridge and in the cirque at the headwaters of South Coldwater Creek. Some pipes include accretionary lapilli near their tops. Lithic clasts in the pipes are up to 6 cm in diameter. The pipes are fines-poor, fragment-supported, "open-work" gravels without matrix. In places, exposures reveal that the pipes originate within the fines-poor tephra of layer A1 and extend upward into A2*, but in other places, they are

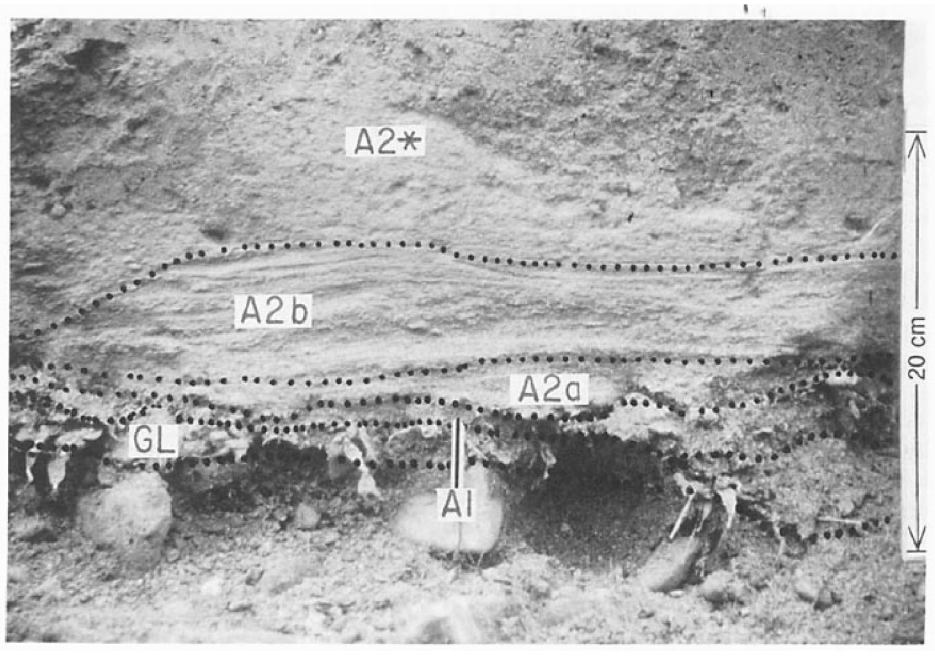

Figure 7. Locality N126.6, 18.5 km from source. Layers A2, A1, and ground layer in tributary of Schultz Creek, overlain by 2-m-thick sequence of A2*. Sequence rests upon terrace gravels. Lower 5 cm is ground layer consisting of tephra mixed with organic material. Layer A1 has crude laminations. Layer A2b shows down-current dune migration in places. Current moved right to left.

Downloaded from gsabulletin.gsapubs.org on May 3, 2012

generated from within layer A2*, as is the case near the mouth of South Coldwater Creek, where layer A2* rests upon avalanche deposits. Less common are gas pipes that extend upward from large individual pieces of charcoal; these formed from smoldering wood.

Many gas pipes end at the surface in small, meter-diameter craters mantled by layer A3. The craters have thin, very localized rims of fine-grained tephra extruded from the pipes. At the base of the slope on the south side of Johnston Ridge, there are large ponds of A2* with hundreds of meter-sized craters (Fig. 8). These small craters show ring-fracture collapse that resulted from loss of tephra from the pipe.

Layer A2* was formed after the passage of the main part of the blast surge (it is underlain by layers A1 and A2). Moreover, the gases within it escaped, probably within a few minutes, but definitely within 1–1.5 hr before layer A3 was emplaced (before 10 a.m. of the same day, Criswell, 1987). The presence of abundant gas pipes in layer A2* in proximal areas and their absence in distal areas such as the Schultz Creek area suggest that the gas pressure within depositing sediments became progressively less during runoff and flow.

Layer A2* is interpreted to have originated by *blocking* resulting from density stratification (Valentine, 1987), and by *drainage* of blast deposits off higher ground (Hoblitt and others, 1981; Fisher and others, 1987) (Fig. 9). Most of the blocking occurred in the proximal zone. For example, it is postulated that by the time the blast surge reached the base of Johnston Ridge (about 3–5 min), a thick, high-concentration (high-density) basal zone of debris had formed by gravity segregation and was blocked by the ridge. This material was then ponded behind levees of the debris avalanche in the North Toutle River Valley (Glicken, 1986). Drainage occurred in lee-side areas in all of the zones. Material from the blast surge parental to layers A1 and A2 drained from steep (>30°–35°) slopes (Fisher and others, 1987) and coalesced as it flowed down valleys. Abundant fines of layer A2 contributed to the lowered permeability and gas-retention ability of the mixture, and layer A1 contributed abundant gases (initially derived from the head of the surge).

UNITS INTERBEDDED WITH A1–A2 LAYERS

There are many stratigraphic sections in which relatively thin, coarse-grained, gray, fines-poor layers occur within, below, above, or between the main units (layers A1, A2a, and A2b). These "added" units between the other layers are interpreted to be locally developed as sug-

Figure 8. Abundant gas-pit craters in ponded A2* deposits 8.4 km northwest of Mount St. Helens. Craters have low rims of tephra projected by escaping gases and also show annular collapse structures caused by subsidence into upper parts of pipes. Photograph taken June 9, 1980. Scale is 60 cm.

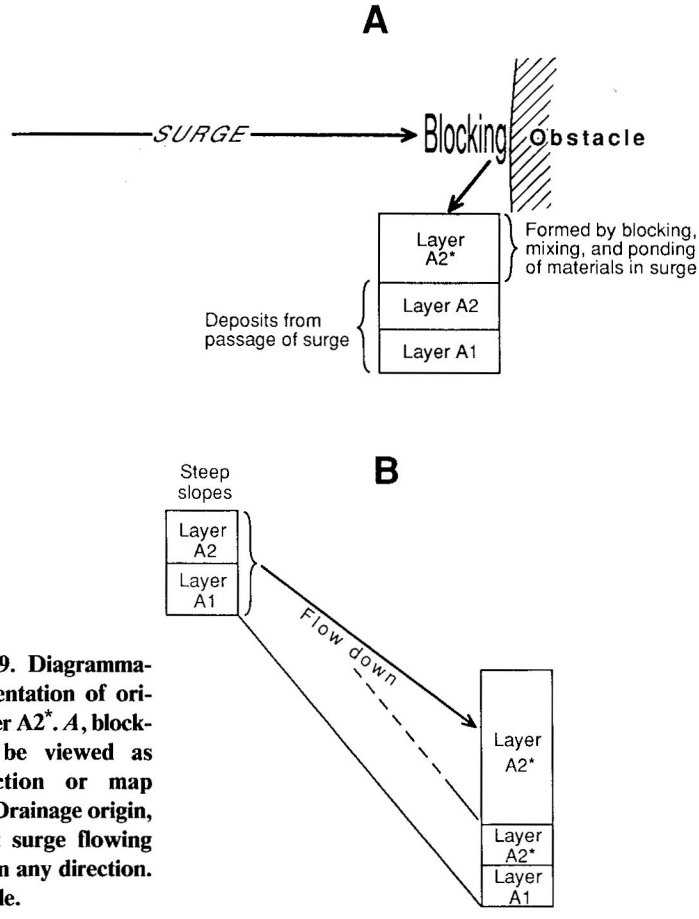

Figure 9. Diagrammatic representation of origins of layer A2*. *A*, blocking; can be viewed as cross section or map view. *B*, Drainage origin, with blast surge flowing downhill in any direction. Not to scale.

Downloaded from gsabulletin.gsapubs.org on May 3, 2012

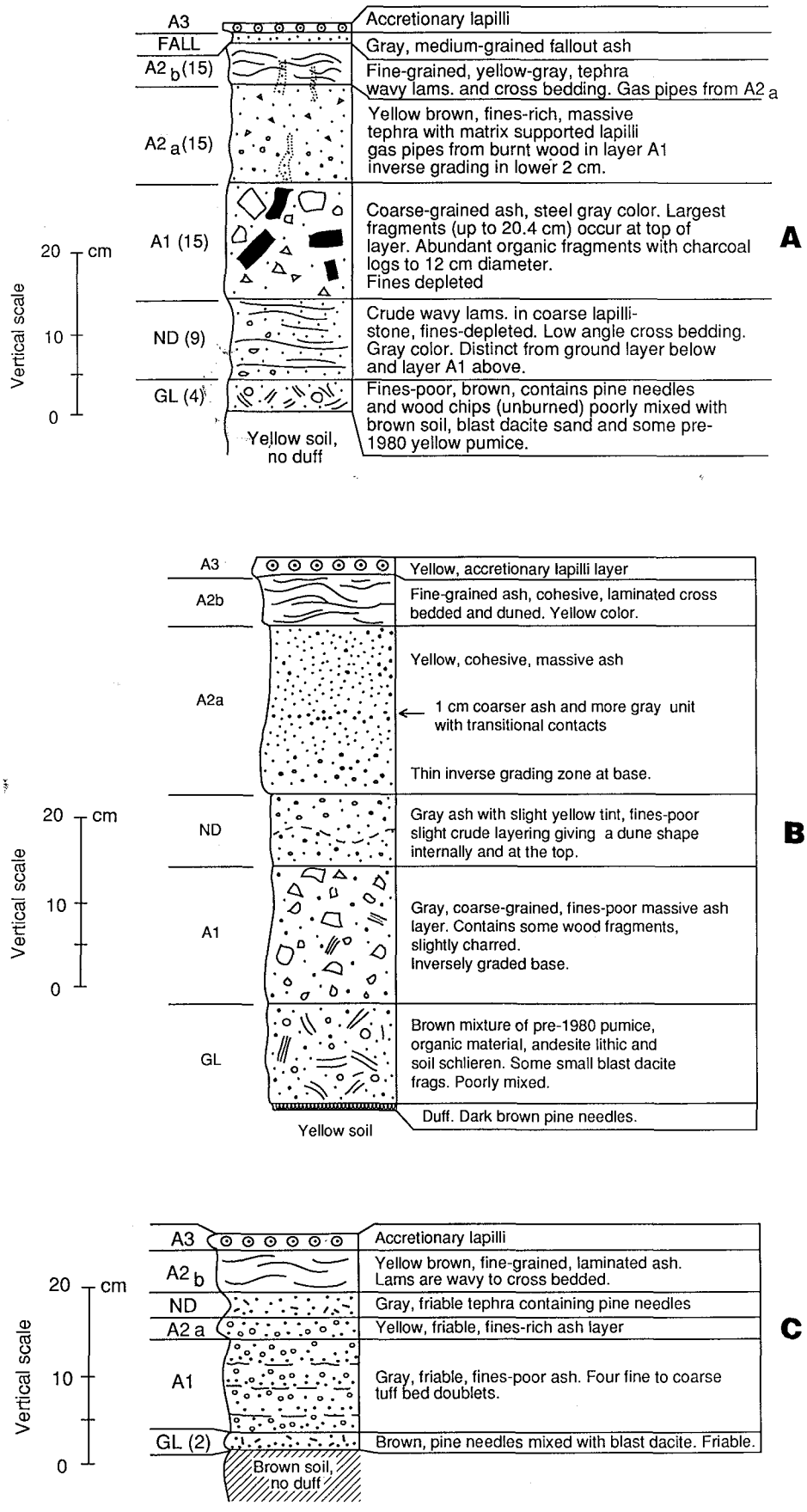

Figure 10. Localities with "added" units. A. Locality E47.5, 9.5 km from source on a horizontal roadbed. The nondesignated (ND) layer between the ground layer and layer A1 is one of the only sections that shows low-angle cross-bedding beneath layer A1. B. Locality E45.5, 10.9 km from source. The nondesignated layer in this section occurs between layers A1 and A2a. It has features characteristic of A1 (that is, fines-poor) and A2 (slight yellow color indicates the presence of fines, and some laminations). C. Locality E15.5, 15.0 km from source. The nondesignated layer at this locality is fines-poor and occurs between layers A2a and A2b.

gested by the fact that they cannot be correlated over large areas. Moreover, these fines-poor units do not occur at a consistent stratigraphic level (Figs. 1 and 10).

Tree blow-down directions show that the lower parts of the blast surge locally flowed in many directions related to topographic configuration—around peaks through low passes, reuniting or crossing one another on opposite sides of a peak, or diverted in downstream directions (Figs. 11a, 11b). In these same areas, the upper parts of the blast surge, which extended above the highest peaks, moved directly across ridges. Thus, it is suggested that the flow moved forward unevenly with overlapping lobes which formed overlapping depositional systems and can explain why there are repeated stratigraphic layers. Repetition of the layers at different stratigraphic levels and the fact that they are not traceable long distances argue for overlap of lobes rather than repeated explosions. In cross-sectional view, vortices that developed in the lee of ridges moved in directions opposite to the main flow (Kieffer, 1981), and as shown herein, also on stoss sides of ridges (Figs. 12a, 12b).

TEXTURE AND STRUCTURES OF DEPOSITS; RELATIONSHIP TO TOPOGRAPHY

Effect of Relief and Surface Roughness

The different widths of the proximal, medial, and distal zones to the east, north, and west of Mount St. Helens (Fig. 1) are directly related to the orientations and heights of ridges and valleys. The blast surge traveled farthest (24 km) to the northwest where the topographic grain, except for the valley side of the North Fork Toutle River, is mostly parallel to the direction of current movement. To the east, the blast surge trav-

Downloaded from gsabulletin.gsapubs.org on May 3, 2012

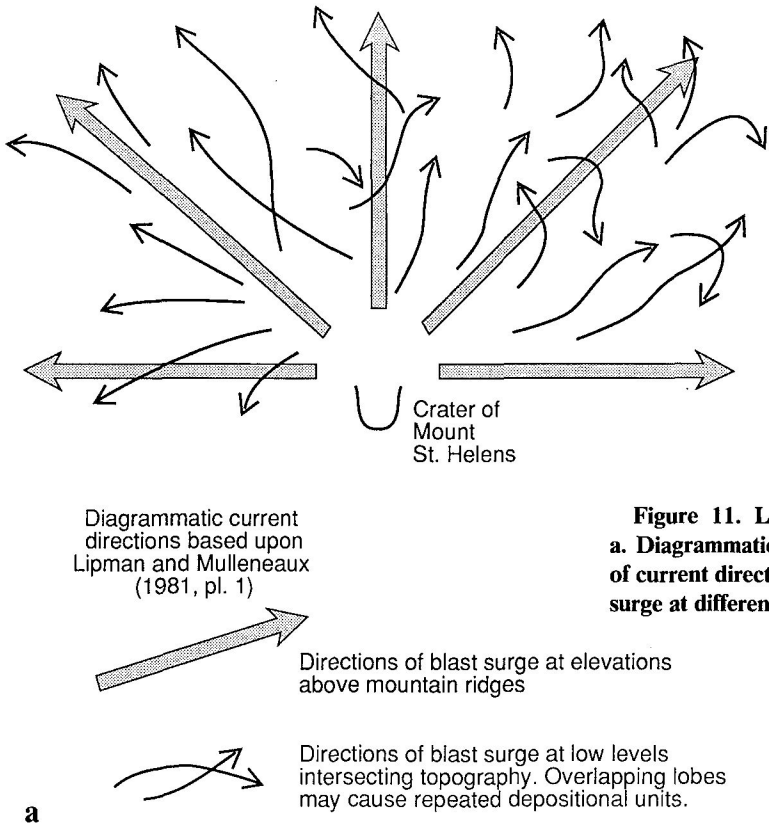

Figure 11. Locality NE48.7. a. Diagrammatic representation of current directions of the blast surge at different elevations.

Figure 11. (*Continued*). b. Blown-down trees crossing at right angles. Those oriented N30°E underlie those oriented N30°W. This indicates that two lobes of the advancing front of the blast surge were deflected around a local topographic high. Left side of photograph is oriented in a northwest direction. Trail in foreground is about 1 m wide. Smooth-cut logs are from trail construction.

eled across three high ridges perpendicular to the current direction for a total distance of only 17 km. To the north, the topographic grain is in part perpendicular and in part parallel to the blast-surge direction. There, the surge traveled an intermediate distance. Thus, the greater the topographic interference, the shorter the length to which the surge traveled.

The effects of topography upon textures and structures is also illustrated by smaller and more local areas such as at localities E55.5 and E56.5 (Fig. 13). Locality E55.5 is 0.9 km east of, and in the lee of, a ridge that overlooks Spirit Lake. It is on a 5° slope 3 m above a logging road (locality E56.5) (Fig. 14). Layer A2 here is thicker than layer A1, but on the horizontal road bed, layer A1 greatly thickens and coarsens.

Rapid lateral changes of deposit characteristics occur on large scales in the blast surge deposit (Fisher and others, 1987) as well as on smaller scales related to small topographic roughness elements (Fig. 14). On the smallest scale, changes in thickness and textures occur across the tops of pre-eruption tree stumps (Fig. 15). A ground layer consisting of tephra mixed with organic matter is overlain by layers A1, A2, and A3 on top of the stump. Each of the layers thins and becomes finer grained away from the lee of the obstacle in the center of the trunk. The surface of deposition on the cut stump is 1.5 m above ground level. The layers are overlain by layer A3 containing accretionary lapilli. The deposits surrounding the stump are considerably thicker than on the stump but show the same stratigraphic sequence.

Depositional units decrease in thickness regionally from proximal to distal zones, but there are wide local variations, which are interpreted to be caused by large velocity fluctuations within the blast surge transport system, owing to high relief and to smaller roughness elements upon the surface of the ground that caused interference with movement of sediment gravity flows during deposition of layers A1 and A2.

Slope Angle and Thickness Ratio

The spread between the highest and the lowest A2/A1 ratios decreases with increase in slope angle, showing that layer A2 thins more rapidly than does layer A1 as slope angle increases (Fig. 16). It thus appears that layer A2 was more mobile than layer A1 and further suggests that the depositional systems which were depositing layers A1 and A2 moved independently of the blast surge and also independently of one another before coming to complete rest. The thickness ratio would remain constant, inde-

Downloaded from gsabulletin.gsapubs.org on May 3, 2012

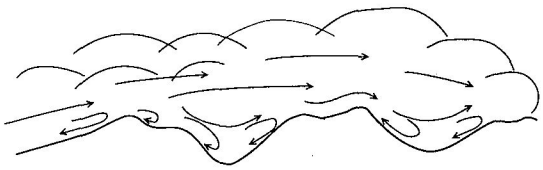

Diagrammatic Vector Directions of Blast Surge

Figure 12a. Diagram of inferred cross-sectional view of vector current directions.

Figure 12b. South-facing slope above Coldwater Lake, 14 km north of Mount St. Helens. View eastward shows blown-down trees pointed uphill in direction of blast surge movement. Cockscomb structure of stump points downhill toward Mount St. Helens.

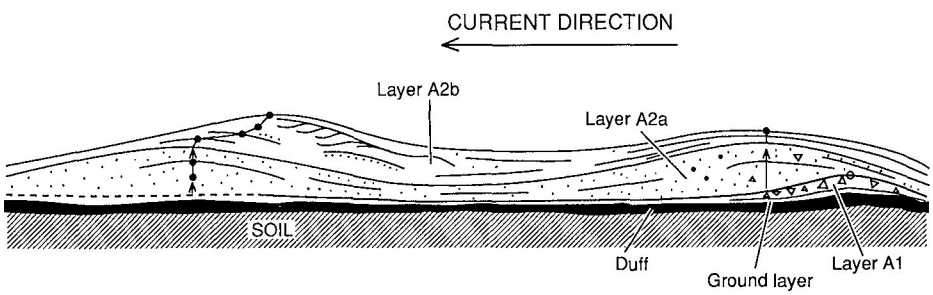

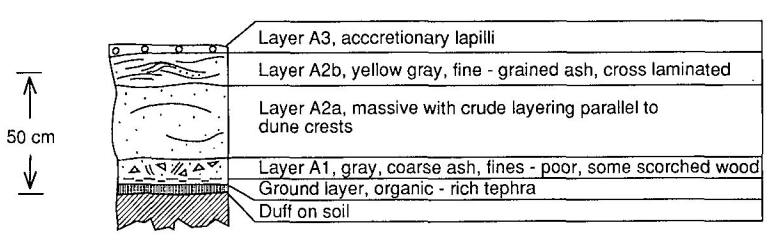

Figure 13. Locality NE55.5, 9.6 km from the volcano. Sketch illustrates the development of dunes on 5° slope on lee side of ridge and shows a layer A2 thicker than layer A1. Connected solid dots illustrate dune crest migration. See text for further description.

pendent of slope angle, if this were not the case.

In addition to the relation of thickness ratios with slope angle, steep slopes facing up-current caused blocking of higher-density, lower parts of stratified flows, a process described by Valentine (1987).

Islands of Nondeposition

Locally, layers A1 and A2 become very thin (a few millimeters) to absent, with layer A3 resting directly upon the ground surface. Two such areas are on ridge tops and are described below. A third area is at the foot of a ridge facing Mount St. Helens. These areas have no distinguishing surface features by which to identify them prior to excavation through layer A3, and it is likely that there are many more such areas.

At locality E46.5 (Fig. 1), there is a flat-topped, 50-m-wide promontory surrounded on three sides by 25° to 30° slopes that extend downward to valleys below, and on a fourth side by a 10° slope extending up from the promontory. The promontory was bulldozed to a flat surface before the eruption for use in logging operations.

On the steep (25°) stoss side about 1 to 2 m below the top of the promontory, the blast-surge deposit is a normal section consisting of a discontinuous ground layer and layers A1 and A2. Where the ground layer is absent, layer A1 rests directly on soil along a sheared contact that has some flame structures.

Across the top of the promontory, the section becomes thinner and finer grained, and the ground layer is absent. Layer A1 pinches and swells between 1.8 and 6 cm thick and wedges out at several places. A2 is laminated, forms dune-shaped bodies (that is, layer A2b). Layer A2a is largely absent. Layer A3 lies above all units and above the pre-eruption surface where surge beds are absent.

About 1 m from the lee-side slope break, there is a tree stump, cut before the eruption, with its cut, flat-top surface standing at 30 cm above the former ground surface. A hole rotted

Downloaded from gsabulletin.gsapubs.org on May 3, 2012

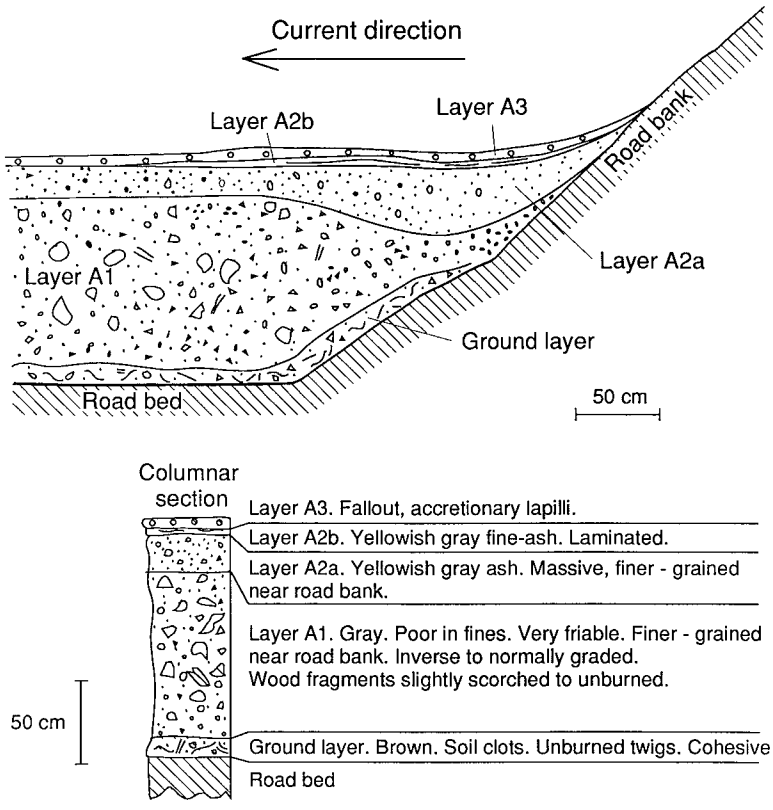

Figure 14. Locality NE56.5, 9.6 km from the volcano. Locality is on roadbed about 20 m from locality NE55.5. Differences between localities of Figures 13 and 14 illustrate the rapid lateral changes in textures and structures caused by interaction of blast surge with small-scale topographic irregularities. Slope of road bank is 21°, which steepens to 38° farther to the right. Layers A1, A2a, and A2b become thinner and finer grained toward steep slope of roadbed independently of one another. Note that layer A2a eroded into top of layer A1 near the break in slope of the road bank where presumably its velocity was greatest. The above relationships indicate that each layer developed from sediment gravity flows which, in turn, drained down the steep slope of the road bank.

downward from the cut surface contains a 20-cm-thick blast surge section consisting of fines-poor layer A1 with blast-dacite fragments to 1.4 cm capped by 0.5 cm of layer A3. Layer A2 is absent. This suggests that the concentration profile of the blast surge that moved across the flat platform was somewhat greater at 30 cm above the ground surface than at ground level, and the hole contains a sample of the blast surge at that level.

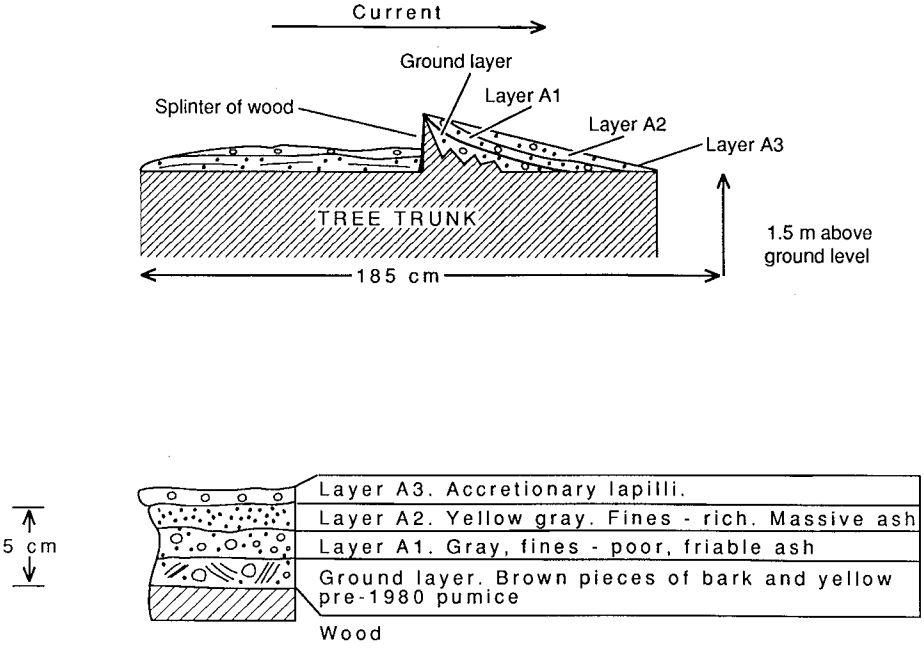

Figure 15. Locality E62.5, on tree stump 15.5 km northeast of volcano. Thin sequence showing the ground layer and layers A1, A2, and A3, 1.5 m above ground level. Tree was cut before May 18, 1980, eruption.

On the crest of a ridge (called here "Smith Creek Ridge" for convenience), there is a thin and discontinuous blast-surge sequence (locality E143.6, Fig. 1). On the ridge crest, layer A1 is lenticular, and A2 is absent. Where both layers are absent, layer A3 rests directly upon soil. On the stoss and lee sides of the ridge, layer A1 is up to 22 cm and is coarser grained than on the top of the ridge. The ground layer beneath A1 is absent from the ridge crest and is discontinuous on the stoss and lee sides, ranging in thickness from 4 cm to zero. The duff beneath the ground layer is lenticular and is thin (3 cm maximum) or absent, indicating erosion by the blast surge prior to development of the ground layer.

Bed Forms

Well-formed bedwaves occur principally in layer A2b as dunes that have internal laminations that are 0.1–1.0 cm thick. Dunes and crossbeds are well formed in many areas of the medial and distal zones, but they also occur in some areas of the proximal zone. With many exceptions, on leeside slopes of 20° or more, crests of dunes commonly migrate uphill (up-current); on lower leeside slopes between about 10° and 20°, the wavy bed-form crests may show migration directions in both up- and down-current directions. With slopes of 10° or less, wavy bed-form crests tend to migrate down-current. An example of up-current migration occurs at E40.5 on a 28° downhill leeside slope (Fig. 17).

Tree blow-down directions and dune-axis orientations are commonly at angles that suggest different flow directions. In places where tree blow-down directions are across slopes, dune axes trend perpendicular to slope, indicating downhill flow in response to gravity (Fig. 18). This relationship suggests that the dunes formed after the depositional system separated from the transport system.

Downloaded from gsabulletin.gsapubs.org on May 3, 2012

GRANULOMETRY

Median and Maximum Diameters versus Distance

Median-diameter data for the sand-size range of blast-surge samples were plotted against distance. The plots show a wide spread of median diameter values nearly as great at local areas within the proximal zone as it is across the full width of the devastated region. This scatter plot is characteristic of the Mount St. Helens blast-surge deposits (Fig. 19), and the same is shown for each layer (Fig. 20). There is, however, a steady decrease in spread between the highest and lowest median diameter values with distance; beyond about 14 to 15 km, the highest and lowest values converge toward a value of between about 2.2 and 2.6 phi. This suggests that maximum particle sizes progressively dropped out of the system, and it is corroborated by the systematic decrease in maximum fragment sizes (Fig. 21). Maximum size data are obtained by measuring the largest diameter of the fragments within a square meter and averaging the values. The ability of the blast surge to transport large clasts thus steadily decreased with distance even though topographic interference caused large local variations.

Grain-Size Parameters and Direction of Transport

Median diameters of the sand-size range plotted against distance for the individual layers

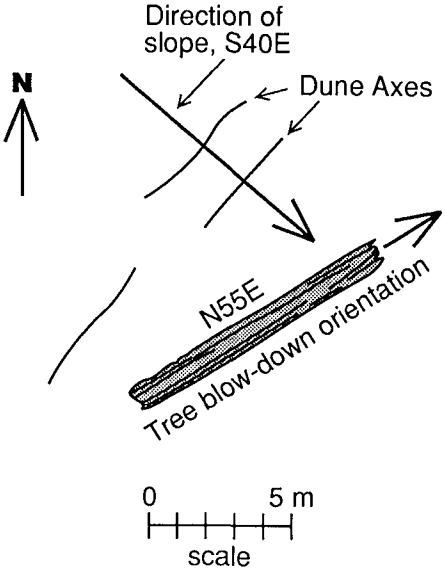

Figure 18. Locality E33.5, 10.3 km from volcano. Plot of tree blow-down orientation (N55°E) across a hillside sloping 20° in a S40°E direction. Dune axes are oriented perpendicular to slope.

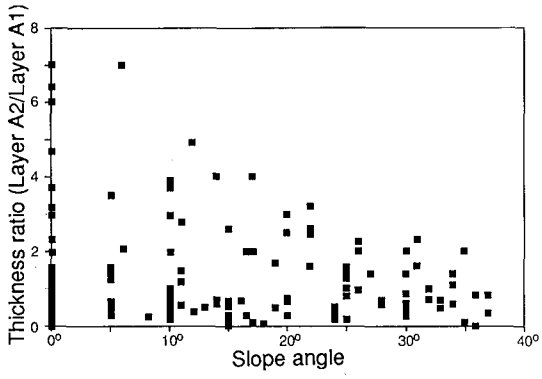

Figure 16. Ratio of thickness of layer A1 to A2 plotted against slope angle. Spread in ratio between highest and lowest values decreases with increases in angle of slope.

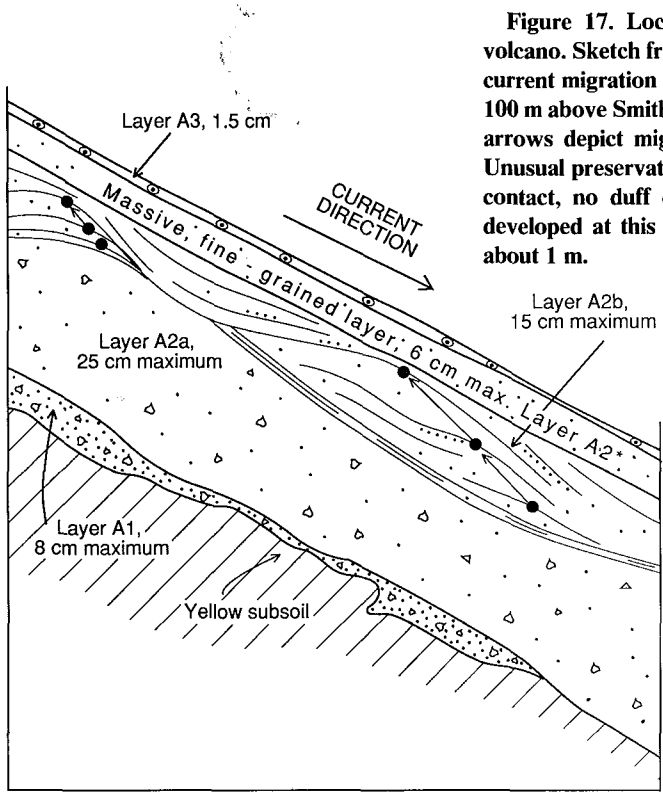

Figure 17. Locality E40.5, 7.8 km from volcano. Sketch from field notes showing up-current migration of dune crests on 28° slope 100 m above Smith Creek. Dots are on crests; arrows depict migration direction of crests. Unusual preservation of layer A2*. Erosional contact, no duff or soil. Ground layer not developed at this place. Length of exposure about 1 m.

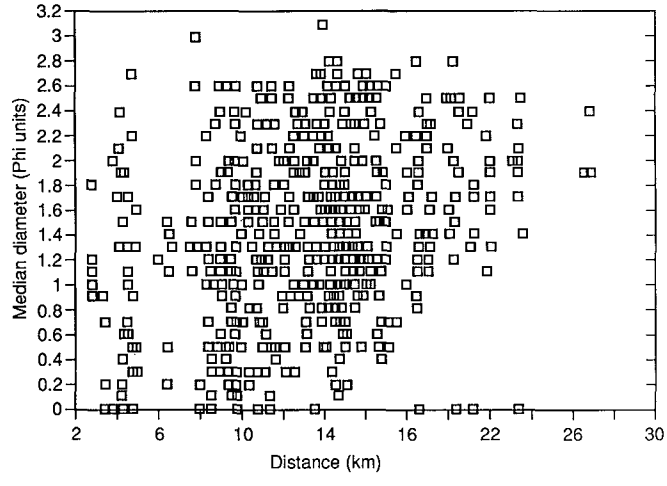

Figure 19. Median diameter values of ash-size (2 mm–1/16 mm) samples of blast surge plotted against distance. Spread in values decrease with distance toward a value between about 2.0 and 2.4 phi.

Downloaded from gsabulletin.gsapubs.org on May 3, 2012

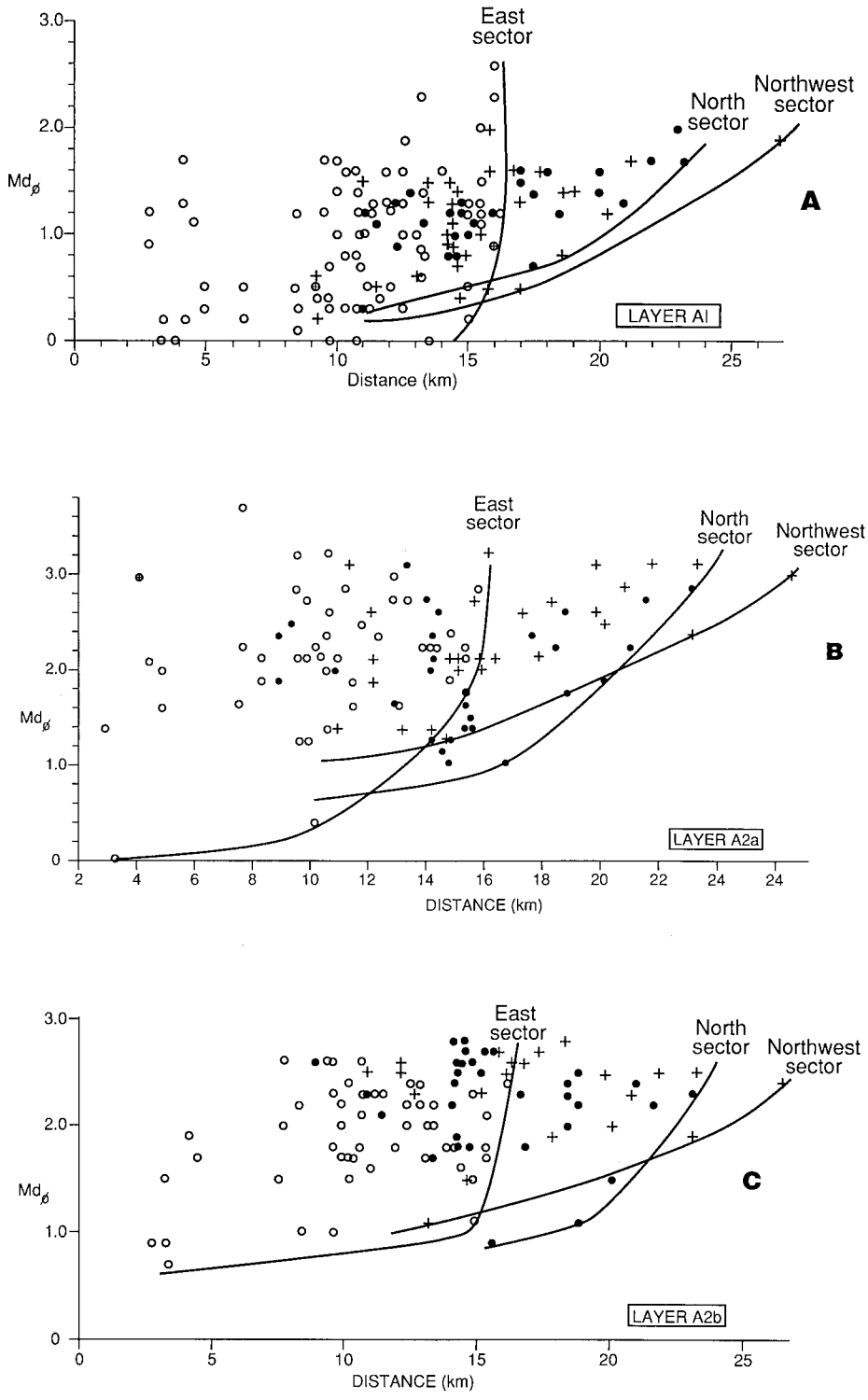

Figure 20. Median diameter versus distance plots for the northwest, north, and east sectors. A. Layer A1. B. Layer A2a. C. Layer A2b. Open circles, samples of east sector; closed circles, samples of north sector; crosses, samples of northwest sector. Lower limiting line for each sector shown. For each plot, the spread in values of median diameter values for the northwest and north sectors decreases with distance.

(A1, A2a, and A2b) (Figs. 20a, 20b, 20c) also show a decrease in spread between highest and lowest median diameter values of sand-size samples. Slopes of lines drawn along lower value limits suggest that the rates at which the sizes decrease with distance are different for different sectors in which the blast surge traveled.

Averages of grain size parameters are arranged according to transect directions away from the source in the approximate directions of movement of the blast surge (Table 1) and these are plotted as Figure 22. The averages, despite the wide range of values shown in Figure 20, are remarkably systematic. Averages of sand-size median diameter (Md_ϕ) arranged vertically in the layers indicate a fining-upward sequence in each of the sector directions. Sand-size sorting parameters (Table 1) also systematically decrease upward. The averaged fine ash percentages systematically increase upward from layer A1 to layer A2b, with the ground layer (Table 1) containing slightly more or slightly less fine ash than layer A1.

The data suggest that there are systematic differences between the three sectors. Samples from the eastern sector have a coarser average value and less fine ash than the northern sector. The same holds true when the northern sector is compared with the northwestern sector. Thus, for Md_ϕ, E SECTOR > N SECTOR > NW SECTOR. For percent fine ash, E SECTOR < N SECTOR < NW SECTOR. Sorting values (Table 1) show little variation.

The wide spread in median-diameter values is believed to be caused by regional and local ground roughness where median-diameter values change over short distances. This may be due to vortices developed in front of, and in back of, obstacles.

CONCLUSIONS

Gravity Segregation and Decoupling of Sediment Gravity Flows

The blast surge deposits at Mount St. Helens developed in three continuous and concurrent stages. The first stage of development was the blast surge, identified here as the *transport system* (Fig. 23). The stratigraphic sequence indicates that the blast surge (1) toppled the trees in directions taken by the lower and most dense part of flow that was directed principally by topography which caused local eddys, (2) formed the ground layer by shear interaction with the ground, and (3) carried fragments from the volcano to the depositional sites. Gravity

Downloaded from gsabulletin.gsapubs.org on May 3, 2012

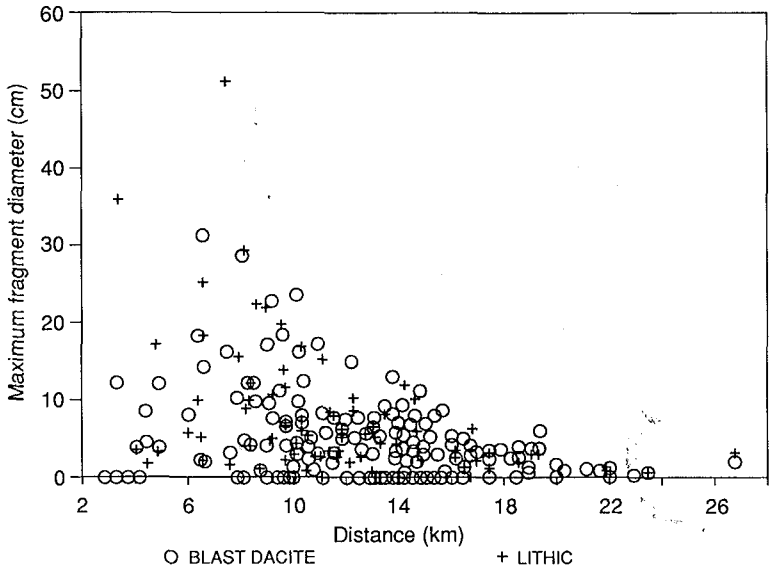

Figure 21. Average diameter of five largest fragments of lithic and blast-dacite fragments plotted against distance from source.

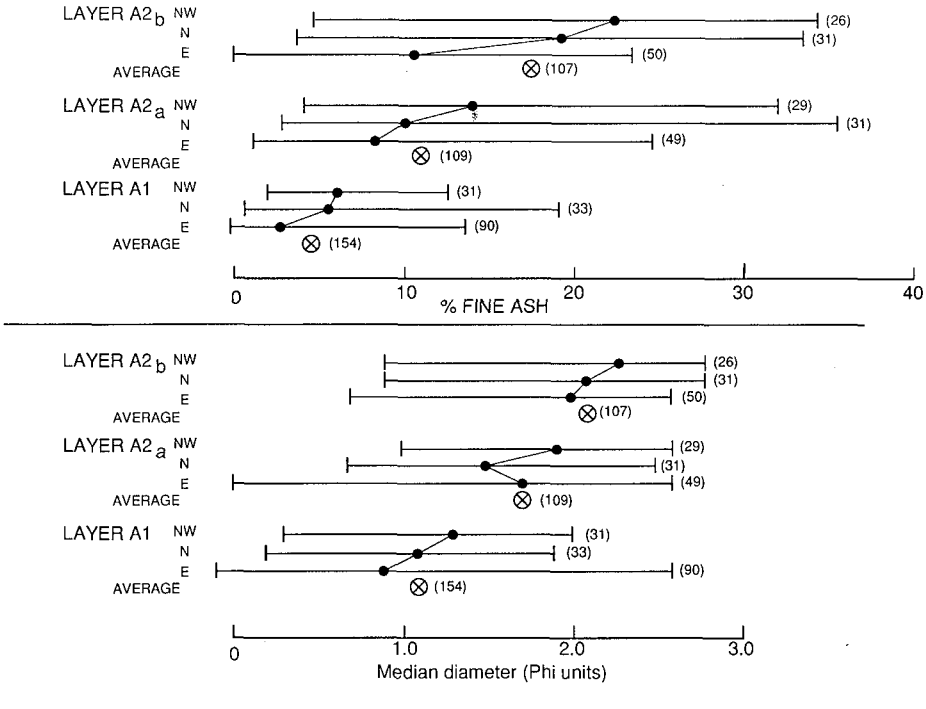

Figure 22. Plots of averages of median diameter and percentage of fine ash (values from Table 1) for layers A1, A2a, and A2b in northwest, north, and east sectors. Bars, range of values for each lobe; heavy dots, average for each lobe; averages of each lobe connected by a line. Circled crosses, averaged values for each layer in all lobes. Numbers in parentheses, number of samples. Plot emphasizes systematic differences of each layer in stratigraphic order.

segregation (Fisher and Heiken, 1982) caused increasing concentration of particles near the basal zone of the surge, resulting in density stratification (Valentine, 1987) and development of the *depositional system.* The depositional system formed two moving sediment gravity flows with independent flow regimes that separated from the transport system and deposited two kinds of layers in succession: (1) first came layer A1 depleted in fines which developed with reverse-to-normal grading as it came to rest and then (2) the overlying finer-grained layer A2.

A sediment gravity flow is one in which gravity acts upon the sediment within the current to drive the flow which carries along the interstitial fluid (Middleton and Hampton, 1976). Grain support is by turbulence, particle collisions, upward-moving fluids and strength of the mass of material. The blast-surge transport system was driven by explosion kinetics within the supersonic zone (Kieffer, 1981) (Fig. 1), but it may have become largely gravity driven within the subsonic zone in medial and distal zones of the devastated area. The depositional system that developed at the base of the blast surge was deposited as layers A1 and A2. These are thought to have been gravity driven in all of the depositional zones because they appear to be controlled by slope angle and direction. They are referred to as "sediment gravity flows." The apparent decoupling of the depositional system from the blast surge is suggested by (1) thickening of beds from high- to low-angle slopes (Fig. 14), (2) the thickness ratio (A2/A1) versus slope angle (Fig. 16), (3) different local directions of tree blow-down orientations and movement directions of layer A2 as indicated by cross-bed and dune-axis orientations (Fig. 18), and (4) thickening of beds behind obstacles (ponding) (Fig. 24).

Independent movement of the sediment gravity flows that deposited layers A1 and A2 is also indicated by reverse grading at the base of each layer, suggesting mass flowage during the last stages of emplacement. Reverse grading is developed during mass movement of high-concentration sediment gravity flows by upward dispersive forces (Bagnold, 1956). The effects of gravity segregation upon the origin of sedimentary features in the Mount St. Helens deposits are similar to some of those described by Lowe (1982) for high-concentration turbidity currents.

Topographic Influences

Topographic irregularities were important controlling factors in (1) the distribution and

Downloaded from gsabulletin.gsapubs.org on May 3, 2012

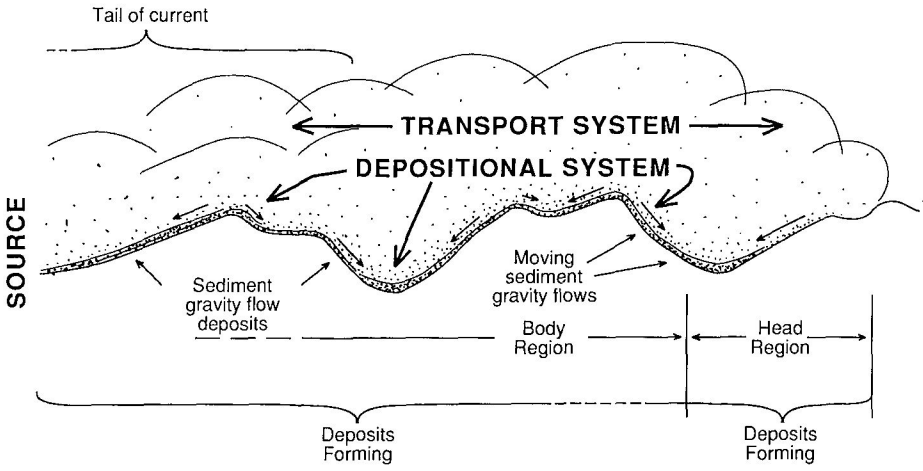

Figure 23. Diagrammatic representation of the transport system and the depositional system. Scouring, formation of the ground layer, and development of sediment gravity flow forming layer A1 occur in the head region followed by development of sediment gravity flows that deposit layer A2 from the body region.

(2) lateral thickness, textural, and structural changes in the Mount St. Helens blast-surge deposits. *Each slope and watershed was a local source for the depositional system.*

Local and regional topographic roughness at all scales caused a wide scatter of median grain size and other grain-size parameters, thickness values, aerial distribution, and differences in length of blast surge travel. The high ridges east of the volcano are perpendicular to flow and acted as baffles, causing considerable resistance to flow (high drag coefficient) and, relative to the other directions, probable greater turbulence in all parts of the blast surge (with consequent greater fines depletion in layers A1 and A2; Table 1). To the northwest, the topographic grain, with ridges essentially parallel to the path of the blast surge, offered the least over-all resistance to flow. To the north, the topographic grain, with high ridges both parallel to, and at right angles to, the blast-surge direction, is intermediate to the other directions. Thus, pre-surge topographic orientation as well as total relief over which a surge moves are important in delineating volcanic hazard zones. Malin and Sheridan (1982), Sheridan and Malin (1983), and McEwen and Malin (1989) have discussed the relationship of topographic relief to flow dispersal. The present study confirms that *topographic relief greatly influences the drag coefficient of flow and that orientation of the topography relative to directions of a decompressing flow importantly affects length of runout.*

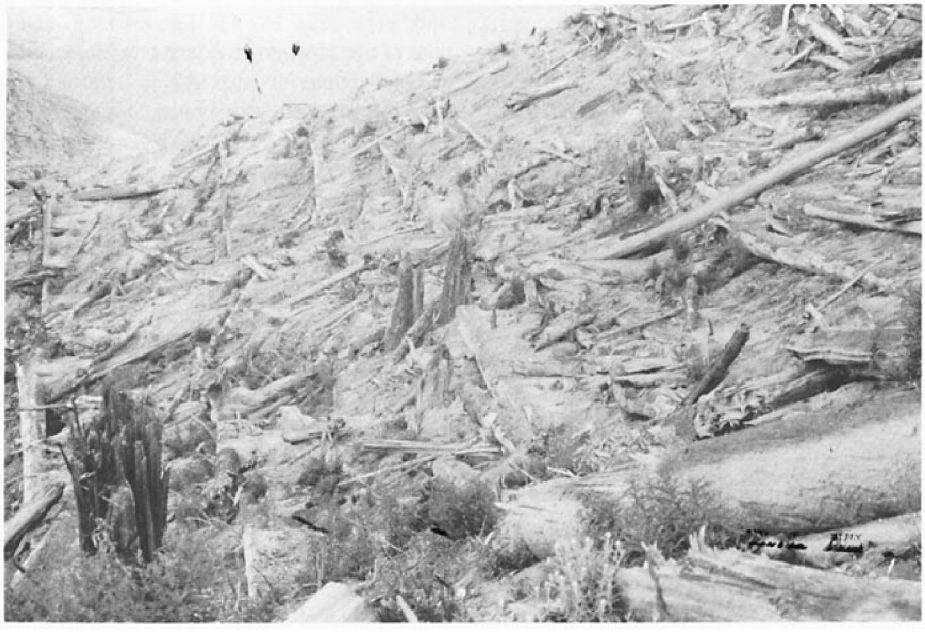

Figure 24. Photograph of area 11.5 km northeast from source. Flat area in background is surface of Spirit Lake. Tree blow-down direction is away from Mount St. Helens and toward the reader. Layers A1 and A2, with layer A3 above them, occur behind trees, indicating downhill drainage toward the source. Reworked ash occurs above layer A3.

Maximum fragment sizes decrease systematically away from the volcano, suggesting that the transport system (blast surge) gradually lost velocity as it moved across the landscape. There are wide variations in size parameters in any local area, however, and these are interpreted to be caused by the influence of small-scale roughness features on lateral size grading within sediment gravity flows of the sediment system which deposited layers A1 and A2. Specific size and thickness parameters in local areas are thus related to (1) initial explosive energy of the blast and the distance from source that the blast surge moved before generating the sediment gravity flows of the depositional system and (2) by local velocity fluctuations of the sediment system caused by local slope angle, topographic irregularities, and other roughness elements (for example, tree stumps, large rocks, and roadcuts). Large to small "sediment traps" containing deposits with large fragments developed in the lee of these roughness elements. Plots of grain size or thickness versus distance therefore result in patterns with wide dispersion in values. It thus appears that such *dispersion patterns are characteristic of deposits of pyroclastic surges and flows deposited across areas of high relief.*

Sedimentological data at Mount St. Helens show that *pyroclastic flows can form in separate basins by topographic blocking of density stratified surges and by draining of surge-generated pyroclastic sediments down slopes to form pyroclastic flows in valleys and ponds* during and after passage of the blast surge. This confirms the idea that pyroclastic flows and pyroclastic surges can form from stratified flows that develop from the passage of turbulent density currents (Valentine, 1987). Deposits of pyroclastic flows found in isolated ponds and valleys across mountain ranges can therefore be explained by the transformation (Fisher, 1983) of surges to flows.

It is now commonly held that moving, ground-hugging, continuous pyroclastic flow sheets can surmount high mountain barriers, and

Downloaded from gsabulletin.gsapubs.org on May 3, 2012

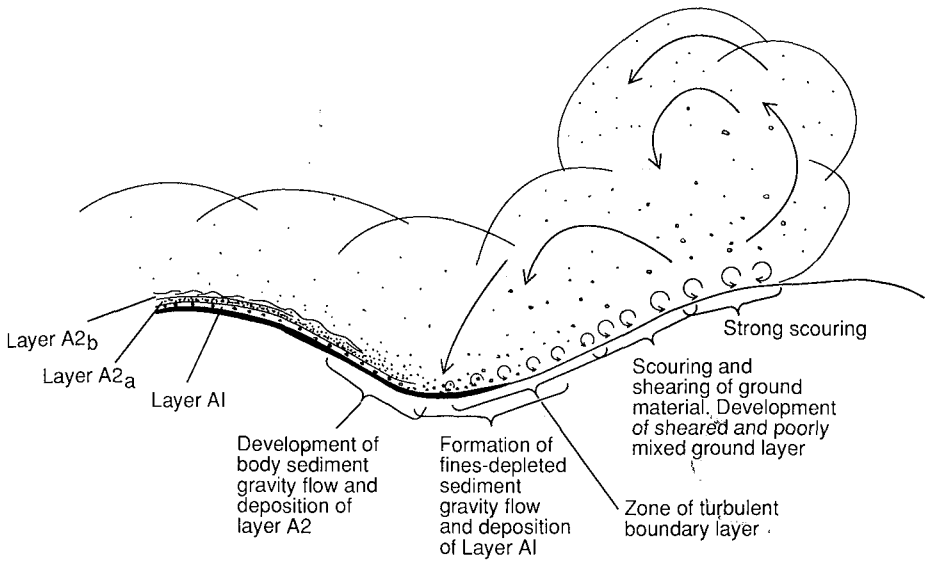

Figure 25. Diagrammatic figure showing principal regions in the blast surge where tree blow-down, scouring, and the gravity-segregated sediment gravity flows that deposited layers A1, A2a, and A2b.

this idea is given credence by mathematical formulations by Sparks and others (1978), showing that flows with velocities of 100 m/s could flow along the ground over barriers as much as 500 m high. Pyroclastic flows, for example, are interpreted to have crossed topographic barriers of 500 m up to nearly 1,000 m (Ito pyroclastic flow, Japan, Yokoyama, 1974; Campanian Ignimbrite, Italy, Barberi and others, 1978; Rosi and others, 1983; pyroclastic flows from Aniakchak and Fisher calderas, Aleutian Islands, Miller and Smith, 1977). The Taupo Ignimbrite, ~30 km^3 in volume, covers more than ~20,000 km^3 and mantles mountains up to 1,500 m higher than the inferred vent as far as 45 km from the source (Wilson and Walker, 1985; Wilson, 1985). Calculations permit the speculation that pyroclastic flows can move along the ground over high mountains as continuous, fast-moving, flowing pyroclastic sheets, but observations at Mount St. Helens suggest that isolated pockets of pyroclastic flows found in separate basins across mountain ranges may also be emplaced from density-stratified turbulent currents.

Interpretation of Flow Dynamics and Depositional Features

The textures, structures, and distribution of the blast surge bedded units suggest the following interpretations of their origins (Fig. 25). As the leading edge of the blast surge moved over the landscape, it first blew down the trees. Behind the leading edge at the base of the blast surge, within a zone of shearing and turbulent scouring, erodable surface materials were partially mixed and sheared in directions of the blast surge movement. Turbulent boundary-layer thickness on the order of 2–20 m is indicated by large furrows on the ground surface in the proximal zone (Kieffer and Sturtevant, 1986, 1988). Vortical flow may have rotated juvenile blast dacite from the head onto the ground surface. In places, some juvenile blast dacite and other materials from the head of the surge entered the turbulent boundary zone and became partially mixed with surface materials and created the ground layer. Beds containing abundant juvenile blast-dacite fragments interbedded with soil-rich layers in the ground layer also suggest the possibility of an early but aerially limited blast-surge pulse that was later overridden by a larger blast which caused the major destruction.

Above the ground layer is layer A1. Its important features are as follows: it is coarse-grained, fines-poor, and commonly reversely to normally graded. The low fines content is interpreted to be caused by winnowing from a turbulent, gas-rich flow head of the blast surge (Fig. 25). Reverse-to-normal grading, commonly caused by dispersive pressure in sediment gravity flows (Fisher and Schmincke, 1984), suggests that the high-concentration mass flow took place during the latter stages of emplacement. Small gas pipes extending across the contact between layer A1 and A2, and large gas pipes in layer $A2^*$, which most likely formed by mixing of layers A1 and A2, provide evidence for a gas-rich layer A1 postulated to have formed from a gas-rich flow head. The material of layer A1 was highly permeable; therefore its gases were quickly lost (1) into the atmosphere or (2) into layer A2 being emplaced above it. Where layers A1 and A2 became mixed to form layer $A2^*$, the gases contributed to the mobility of the moving layer $A2^*$ but were quickly lost after deposition through development of gas pipes.

The fines-poor layer A1 is similar to, and probably formed in the same way (that is, the flow head) as, layer 1H of the ignimbrite sequence at Taupo, New Zealand (Walker and others, 1981; Wilson and Walker, 1985; Wilson, 1985), but at Taupo, it is called a ground layer. At Mount St. Helens, the fines-poor layer (A1) occurs *above* a ground layer. The ground layer at Mount St. Helens is interpreted to have developed by the interaction of the surge with the ground surface, rather than deposited from the flow head of the blast surge.

As the sediment gravity-flow parent to layer A1 slowed or came to rest, another sediment gravity flow, parent to layer A2, began forming and flowed on top of it. Gases being expelled from layer A1 may have mixed with materials of A2 as it flowed and contributed to its mobility. In proximal areas, layer A2 is commonly a single massive layer, but in medial and distal areas, the lower massive part (A2a) is overlain by a laminated or thinly bedded upper part (A2b) showing cross-bedding and dunes. The upper part of layer A2 is interpreted as being deposited from traction currents of dilute tails of the waning currents of the depositional system.

Many sections have fines-depleted layers or repeated layer A2 doublets within the normal A1–A2 depositional framework. It is suggested that the simple A1–A2 stratigraphy was interrupted by deposition from overlapping lobes that developed at the front of the flow, and probably within it, and moved in different directions because of topographic interference. The additional units can also be interpreted as caused by successive explosions during early stages of the eruption, but because the units cannot be correlated over large areas, independent evidence of multiple explosions after development of the ground layer is absent.

In areas of slopes >30°–35°, the sediment gravity flows, parents to layers A1 and A2, flowed together and mixed while moving downhill into depressions, and down valleys as high-concentration pyroclastic flows (layer $A2^*$). These secondary pyroclastic flows were rich in gases derived from the surge head. Greater abundance of gas pipes and small gas pits in proximal than in distal areas, especially at the base of volcano-facing (south) slopes, suggests that materials being deposited from the

Downloaded from gsabulletin.gsapubs.org on May 3, 2012

blast surge were very mobile. Deposition was so rapid that pressurized gases were trapped, but degassing was largely finished by 10 a.m., May 18, when the accretionary lapilli of layer A3 had fallen. In a tributary of Schultz Creek (locality N126.6), where layer A2* is 2 m thick, there are no gas pipes. This is interpreted to be from gas loss during travel down-valley prior to deposition.

The wide scatter of grain-size values with distance is an expected result of surge and flow layers deposited in areas of rugged relief. Wide local variations in grain-size values of the blast surge deposits at Mount St. Helens are not surprising, considering (1) the great influence of topography on velocity of the blast surge, (2) the complexities of turbulent vortices within the blast surge, and (3) the formation of two sets of independent sediment gravity flows (forming layers A1 and A2) derived from the transport system and controlled by local topography.

Kieffer (1981) and Kieffer and Sturtevant (1988) indicated that the blast surge initially advanced at supersonic velocities. This is also suggested by the intensity of erosion of the substrate defining the zonal proximal, medial, and distal boundaries which, in part, approximately mimic the shape of the boundary between supersonic and subsonic flow calculated by Kieffer (1981). *The main sedimentological influence of subsonic and supersonic flow, therefore, appears to have been upon how the material was areally distributed by the blast surge, and the severity of erosion of the surface underlying flow.*

ACKNOWLEDGMENTS

The U.S. Geological Survey, Johnston Cascade Volcano Observatory, Vancouver, Washington, is gratefully acknowledged for logistical support with special thanks to Dick Janda, Don Peterson, Norm Macleod, Don Swanson, Rick Hoblitt, and Bobbie Meyers. Harry Glicken, Ph.D. student at University of California, Santa Barbara, with extensive experience at the May 18, 1980, Mount St. Helens eruption site, was a valuable guide to many aspects of the field work. The able assistance in the field and discussions with Greg Valentine (1985), Michael Ort (1986), and David Buesch (1987), Ph.D. students at UCSB, are very much appreciated. Much of the data analysis was done in France during part of a sabbatical leave from UCSB in 1988, and I would like to thank the faculty and staff at the University of Clermont-Ferrand, especially Pierre Vincent and Philippe Vidal, for providing the opportunity to study in France. I extend thanks to those who visited me at Cispus Environmental Center for their company, discussions, and accompanying me on field excursions. For accommodations, friendship, and gracious help at Cispus Environmental Center—Jeannette Woodruff, Jim Garnett, and Pamela Pollman—I give thanks. David Buesch, Harry Glicken, Michael Ort, Greg Valentine, and three anonymous reviewers made helpful suggestions on the manuscript. Funding by National Science Foundation Grant EAR86-05135 was indispensable for completion of the study.

REFERENCES CITED

Bagnold, R. A., 1956, The flow of cohesionless grains in fluids: Royal Society of London Philosophical Transactions, ser. A, v. 249, p. 235–297.

Barberi, F., Innocenti, F., Lirer, L., Munno, R., Pescatore, T., and Santacroce, R., 1978, The Campanian ignimbrite: A major prehistoric eruption in the Naples area (Italy): Bulletin Volcanologique, v. 41, p. 10–31.

Brantley, S. R., and Waitt, R. B., 1988, Interrelations among pyroclastic surge, pyroclastic flow, and lahars in Smith Creek valley during first minutes of 18 May 1980 eruption of Mount St. Helens, USA: Bulletin of Volcanology, v. 50, p. 304–326.

Criswell, C. W., 1987, Chronology and pyroclastic stratigraphy of the May 18, 1980, eruption of Mount St. Helens, Washington, Journal of Geophysical Research, v. 92, p. 10237–10266.

Evarts, R. C., Ashley, R. P., and Smith, J. G., 1987, Geology of the Mount St. Helens area: Record of discontinuous volcanic and plutonic activity in the Cascade arc of southern Washington: Journal of Geophysical Research, v. 92, p. 10155–10169.

Fisher, R. V., 1983, Flow transformations in sediment gravity flows: Geology, v. 11, p. 273–274.

Fisher, R. V., and Heiken, G. H., 1982, Mt. Pelée, Martinique: May 8 and 20 pyroclastic flows and surges: Journal of Volcanology and Geothermal Research, v. 13, p. 339–371.

Fisher, R. V., and Schmincke, H.-U., 1984, Pyroclastic rocks: Berlin, Heidelberg, New York, Tokyo, Springer-Verlag, 472 p.

Fisher, R. V., Glicken, H. X., and Hoblitt, R. P., 1987, May 18, 1980, Mount St. Helens deposits in South Coldwater Creek, Washington: Journal of Geophysical Research, v. 92, p. 10267–10283.

Glicken, H., 1986, Rockslide-debris avalanche of May 18, 1980, Mount St. Helens Volcano, Washington [Ph.D. dissert.]: Santa Barbara, California, University of California, 303 p.

Glicken, H., in press, Rockslide-debris avalanche of May 18, 1980, Mount St. Helens Volcano, Washington: U.S. Geological Survey Professional Paper 1488.

Hoblitt, R. P., 1988, Was the deposit of the May 18, 1980, direct blast at Mount St. Helens, Washington, produced by two separate pulses?: International Association of Volcanology and Chemistry of the Earth's Interior Workshop, Guadeloupe and Martinique, March 6–16, 1988, Abstracts Volume, p. 16.

——1989, Evidence for two explosions in the May 18, 1980, lateral blast at Mount St. Helens, Washington: Continental Magmatism Abstracts, New Mexico Institute of Mining and Mineral Resources Bulletin 131, p. 131.

Hoblitt, R. P., Miller, C. D., and Vallance, J. W., 1981, Origin and stratigraphy of the deposit produced by the May 18 directed blast, *in* Lipman, P. W., and Mullineaux, D. R., eds., The 1980 eruptions of Mount St. Helens, Washington: U.S. Geological Survey Professional Paper 1250, p. 401–419.

Kieffer, S. W., 1981, Fluid dynamics of the May 18 blast at Mount St. Helens, *in* Lipman, P. W., and Mullineaux, D. R., eds., The 1980 eruptions of Mount St. Helens, Washington: U.S. Geological Survey Professional Paper 1250, p. 379–400.

Kieffer, S. W., and Sturtevant, B., 1986, Erosional furrows formed during the lateral blast at Mount St. Helens, May 18, 1980: Indicators of longitudinal vortices in the boundary layer: International Volcanological Congress, New Zealand, Abstracts, p. 59.

——1988, Erosional furrows formed during the lateral blast at Mount St. Helens, May 18, 1980: Journal of Geophysical Research, v. 93, p. 14793–14816.

Lipman, P. W., and Mullineaux, D., eds., 1981, The 1980 eruptions of Mount St. Helens: U.S. Geological Survey Professional Paper 1250, p. 1–844.

Lowe, D. R., 1982, Sediment gravity flows: II. Depositional models with special reference to the deposits of high-density turbidity currents: Journal of Sedimentary Petrology, v. 52, p. 279–297.

Malin, M. C., and Sheridan, M. F., 1982, Computer assisted mapping of pyroclastic surges: Science, v. 217, p. 637–639.

McEwen, A. S., and Malin, M. C., 1989, Dynamics of Mount St. Helens' pyroclastic flows, rockslide-avalanche, lahars, and blast: Journal of Volcanology and Geothermal Research, v. 37, p. 205–231.

Middleton, G. V., and Hampton, M. A., 1976, Subaqueous sediment transport and deposition by sediment gravity flows, *in* Stanley, D. J., and Swift, D.J.P., eds., Marine sediment transport and environmental management: New York, John Wiley and Sons, Inc., p. 197–218.

Miller, T. P., and Smith, R. L., 1977, Spectacular mobility of ash flows around Aniakchak and Fisher calderas, Alaska: Geology, v. 5, p. 173–176.

Moore, J. G., and Rice, C. J., 1984, Chronology and character of the May 18, 1980, explosive eruption of Mount St. Helens, *in* Explosive volcanism: Inception, evolution, hazards: Washington, D.C., National Academy Press, p. 133–142.

Moore, J. G., and Sisson, T. W., 1981, Deposits and effects of the May 18 pyroclastic surge, *in* Lipman, P. W., and Mullineaux, D. R., eds., The 1980 eruptions of Mount St. Helens, Washington: U.S. Geological Survey Professional Paper 1250, p. 421–438.

Rosi, M., Sbrana, A., and Principe, C., 1983, The Phlegraean Fields: Structural evolution, volcanic history and eruptive mechanisms, *in* Sheridan, M. F., and Barberi, F., eds., Explosive volcanism: Journal of Volcanology and Geothermal Research, v. 17, p. 89–109.

Sheridan, M. F., and Malin, M. C., 1983, Application of computer-assisted mapping to volcanic hazard evaluation of surge eruptions: Vulcano, Lipari, and Vesuvius: Journal of Volcanology and Geothermal Research, v. 17, p. 187–202.

Sisson, T. W., 1982, Sedimentary characteristics of the airfall deposit produced by the major pyroclastic surge of May 18, 1980, at Mount St. Helens, Washington [M.A. dissert.]: Santa Barbara, California, University of California at Santa Barbara, 145 p.

Sparks, R.S.J., Wilson, L., and Hulme, G., 1978, Theoretical modeling of the generation, movement and emplacement of pyroclastic flows by column collapse: Journal of Geophysical Research, v. 83, p. 1727–1739.

Sparks, R.S.J., Moore, J. G., and Rice, C. J., 1986, The initial giant umbrella cloud of the May 18th, 1980, explosive eruption of Mount St. Helens: Journal of Volcanology and Geothermal Research, v. 28, p. 257–274.

Valentine, G. A., 1987, Stratified flow in pyroclastic surges: Bulletin of Volcanology, v. 49, p. 616–630.

Voight, B., 1981, Time scale for the first movements of the May 18 eruption, *in* Lipman, P. W., and Mullineaux, D. R., eds., The 1980 eruptions of Mount St. Helens, Washington: U.S. Geological Survey Professional Paper 1250, p. 69–86.

Voight, B., Glicken, H., Janda, R. J., and Douglass, P. M., 1981, Catastrophic rockslide avalanche of May 18, *in* Lipman, P. W., and Mullineaux, D. R., eds., The 1980 eruptions of Mount St. Helens, Washington: U.S. Geological Survey Professional Paper 1250, p. 347–377.

Voight, B., Janda, R. J., Glicken, H., and Douglass, P. M., 1983, Nature and mechanics of the Mount St. Helens rockslide-avalanche of 18 May 1980: Geotechnique, v. 33, p. 24.

Waitt, R. B., Jr., 1981, Devastating pyroclastic density flow and attendant air fall of May 18—Stratigraphy and sedimentology, *in* Lipman, P. W., and Mullineaux, D. R., eds., The 1980 eruptions of Mount St. Helens, Washington: U.S. Geological Survey Professional Paper 1250, p. 601–616.

Walker, G.P.L., Self, S., and Froggatt, P. C., 1981, The ground layer of the Taupo Ignimbrite: A striking example of sedimentation from a pyroclastic flow: Journal of Volcanology and Geothermal Research, v. 10, p. 1–11.

Wilson, C.J.N., 1985, The Taupo eruption, New Zealand II. The Taupo Ignimbrite: Royal Society of London Philosophical Transactions, ser. A 314, p. 229–310.

Wilson, C.J.N., and Walker, G.P.L., 1985, The Taupo eruption, New Zealand I. General aspects: Royal Society of London Philosophical Transactions, ser. A 314, p. 199–228.

Yokoyama, S., 1974, Mode of movement and emplacement of Ito pyroclastic flow from Aira Caldera, Japan: Science Reports of Tokyo Kyoiku Daigaku Sec C (Geography, Geology and Mineralogy), v. 12, p. 17–62.

Manuscript Received by the Society May 26, 1989
Revised Manuscript Received December 19, 1989
Manuscript Accepted December 28, 1989